Journal of Engineering Mathematics **37:** 129–142, 2000.

Flow induced surface switching in a bistable nematic device

J. G. McINTOSH and F. M. LESLIE
Department of Mathematics, University of Strathclyde, Livingstone Tower, 26 Richmond Street, Glasgow, Scotland, UK; e-mail: caar34@strath.ac.uk e-mail: caas01@strath.ac.uk

Received 5 February 1999; accepted in revised form 26 July 1999

Abstract. A surprising feature of liquid crystals is that rapid changes in alignment in these anisotropic liquids can induce significant flow, termed backflow, which in turn influences the alignment. A recent paper has suggested that such backflow may be the mechanism behind the fast switching observed in certain bistable nematic cells on the application of electric fields. In these experiments a weakly chiral nematic with unequal monostable surface anchorings is switched rapidly between a uniform and a π-twist configuration, and it is conjectured that the backflow induced initially at the more strongly anchored surface plays a crucial role in the switching process. In this paper continuum theory is employed for nematic liquid crystals to investigate this phenomenon, and confirms that backflow can play an important role in the switching.

Key words: nematic, surface-controlled bistable device, backflow, weak and strong anchoring

1. Introduction

It has been known from very early this century that flow can influence the alignment of a nematic liquid crystal, and indeed flow was frequently used to align nematics in cells. However, the realisation that changes in alignment can induce flow came more recently, this emanating from research into liquid-crystal display devices in the 1970s. Gerritsma, van Doorn and van Zanten [1] observed a non-monotonic decrease in light transmitted through a nematic cell following the removal of the applied voltage, which they termed optical bounce. This they correctly attributed to an induced flow effect, van Doorn [2, 3] and Berreman [4] confirming their explanations by appropriate numerical integrations of the continuum equations for nematic liquid crystals.

Such induced flow, or backflow as it is commonly called, was initially regarded as something that one should seek to minimise in order to avoid undue complications in display devices, but apart from a few studies this phenomenon has not received the attention it merits. However, in the last few years there has been a renewal of interest in the development of fast-switching nematic displays, largely through the exploitation of different surface effects (see for example [5, 6]), and in a recent paper Dozov, Nobili and Durand [7] describe experiments in which they employ electric fields to switch rapidly a bistable nematic cell with weak, unequal monostable surface anchorings. A key element in their switching mechanism they attribute to backflow induced initially at the plate with the stronger anchoring, and this has subsequently been confirmed by an appropriate theoretical study [8]. In this paper we pursue our investigation of this topic, and present further numerical solutions of the relevant continuum equations that support our preliminary results.

The following section gives an outline of the necessary continuum equations proposed by Ericksen [9] and Leslie [10] for nematic liquid crystals. There follows an illustration of

backflow in a rather simple context that allows a relatively straightforward analysis of the effect, this very similar to one given earlier by Clark and Leslie [11]. Thereafter we turn to the main topic of our paper and obtain further solutions relevant to the experiment by Dozov and co-workers.

Full accounts of properties of nematic liquid crystals are available in the books by Prost and de Gennes [12] and Chandrasekhar [13, Chapter 3], but a compact introduction to the continuum theory for these anisotropic liquids can be found in a recent article by Leslie [14].

2. Continuum theory

In many situations a nematic liquid crystal can be regarded as an incompressible, transversely isotropic liquid, and thus in addition to the velocity vector **v** one requires simply a unit vector field, or director, **n** to describe the orientation of the local axis of anisotropy, the two variables subject to the constraints

$$v_{i,i} = 0, \qquad n_i n_i = 1. \tag{1}$$

Here it is convenient to employ Cartesian tensor notation, so that a comma preceding a suffix denotes partial differentiation with respect to the corresponding spatial coordinate, and the summation convention applies.

The continuum theory proposed for these anisotropic liquids by Ericksen [9] and Leslie [10] adopts these constraints and essentially employs the balance laws for linear and angular momentum, the latter expanded to include explicit body and surface moments (see, for example, Leslie [15]). For present purposes these equations are most conveniently expressed in terms of three scalar functions, an elastic stored energy W, a dissipation function D, and, should an electric or magnetic field be present, an associated electric or magnetic energy U. In this event, the balance of linear momentum takes the form [16]

$$\rho \dot{v}_i = \left(\frac{\partial D}{\partial v_{i,j}} \right)_{,j} - \frac{\partial D}{\partial \dot{n}_k} n_{k,i} - p_{,i}, \tag{2}$$

where ρ denotes density, p an undetermined pressure, and the superposed dot the material time derivative, while the balance of angular momentum is given by

$$\left(\frac{\partial W}{\partial n_{i,j}} \right)_{,j} - \frac{\partial W}{\partial n_i} - \frac{\partial D}{\partial \dot{n}_i} + \frac{\partial U}{\partial n_i} = \gamma n_i, \tag{3}$$

in which γ is an arbitrary scalar. The elastic energy W is the Frank–Oseen energy [17, 18]

$$\begin{aligned} 2W \;=\; & K_1 (n_{k,k})^2 + K_2 (n_k e_{kpq} n_{q,p})^2 + K_3 n_{k,p} n_p n_{k,q} n_q \\ & + (K_2 + K_4)(n_{k,p} n_{p,k} - (n_{k,k})^2), \end{aligned} \tag{4}$$

the K's constant coefficients. The dissipation function D can be expressed as [15, 19]

$$\begin{aligned} 2D \;=\; & \alpha_1 (n_k D_{kp} n_p)^2 + \alpha_4 D_{kp} D_{kp} + (\alpha_5 + \alpha_6) D_{kp} n_p D_{kq} n_q \\ & + (\alpha_3 - \alpha_2) N_k N_k + 2(\alpha_3 + \alpha_2) N_k D_{kp} n_p, \end{aligned} \tag{5}$$

the α's constant coefficients, and

$$2D_{ij} = v_{i,j} + v_{j,i}, \qquad 2W_{ij} = v_{i,j} - v_{j,i}, \qquad N_i = \dot{n}_i - W_{ip}n_p. \tag{6}$$

The above expression assumes the Parodi relation [20] between the viscous coefficients, namely

$$\alpha_2 + \alpha_3 = \alpha_6 - \alpha_5. \tag{7}$$

Finally the electric energy U is the familiar

$$2U = D_k E_k = \varepsilon_0 E_k E_k + \varepsilon_a (E_k n_k)^2, \tag{8}$$

where **E** and **D** are the electric field and displacement, respectively, and ε_0 and ε_a are dielectric permittivities. An analogous expression is valid for a magnetic field.

In the following sections we consider solutions of the above equations in which the director **n**, velocity **v** and electric field **E** take the forms referred to Cartesian axes

$$\begin{aligned} n_x &= \sin\theta(z,t), \qquad n_y = 0, \qquad n_z = \cos\theta(z,t), \\ v_x &= u(z,t), \qquad v_y = v_z = 0, \\ E_x &= E_y = 0, \qquad E_z = E. \end{aligned} \tag{9}$$

Thus, with a prime and a superposed dot denoting partial derivatives with respect to z and t, respectively,

$$W = \mathcal{W}(\theta, \theta'), \qquad D = \Delta(u', \theta, \dot{\theta}), \qquad U = \mathcal{X}(\theta, E), \tag{10}$$

and as discussed by Ericksen [16] the Equations (2) and (3) may be recast as

$$\rho\dot{u} = \left(\frac{\partial\Delta}{\partial u'}\right)', \qquad \left(\frac{\partial\mathcal{W}}{\partial\theta'}\right)' - \frac{\partial\mathcal{W}}{\partial\theta} - \frac{\partial\Delta}{\partial\dot{\theta}} + \frac{\partial\mathcal{X}}{\partial\theta} = 0, \tag{11}$$

along with an expression for the pressure. Also a rather straightforward calculation yields

$$2\mathcal{W} = f(\theta)(\theta')^2, \quad f(\theta) = K_1 \sin^2\theta + K_3 \cos^2\theta, \tag{12}$$

$$2\mathcal{X} = \varepsilon(\theta)E^2, \quad \varepsilon(\theta) = \varepsilon_0 + \varepsilon_a \cos^2\theta, \tag{13}$$

$$\begin{aligned} 2\Delta &= g(\theta)(u')^2 + \gamma_1(\dot{\theta})^2 + 2m(\theta)u'\dot{\theta}, \quad \gamma_1 = \alpha_3 - \alpha_2, \\ 2g(\theta) &= \alpha_4 + (\alpha_5 - \alpha_2)\cos^2\theta + (\alpha_3 + \alpha_6 + 2\alpha_1\cos^2\theta)\sin^2\theta, \\ m(\theta) &= \alpha_2 \cos^2\theta - \alpha_3 \sin^2\theta. \end{aligned} \tag{14}$$

Given the elastic energy and the dissipation function must both be positive definite, it follows that one must have

$$f(\theta) > 0, \qquad g(\theta) > 0, \qquad \gamma_1 > 0, \qquad \gamma_1 g(\theta) - m^2(\theta) > 0. \tag{15}$$

Finally, combining Equations (11)–(14), one obtains

$$\rho\dot{u} = \left(g(\theta)u' + m(\theta)\dot{\theta}\right)', \tag{16}$$

and

$$2f(\theta)\theta'' + \frac{\mathrm{d}f(\theta)}{\mathrm{d}\theta}(\theta')^2 - 2\gamma_1\dot{\theta} - 2m(\theta)u' - 2\varepsilon_a E^2 \sin\theta\cos\theta = 0, \tag{17}$$

which we return to below.

3. Orientational relaxation at a single boundary

Before turning to the more complex response of a nematic in a thin cell between two parallel plates with unequal anchoring strengths, we believe it may be helpful to look first at the rather simpler situation of a nematic strongly anchored at a single boundary, this assuming a large gap between the plates so that one can essentially ignore any interaction between effects emanating from them. For a nematic with positive dielectric anisotropy, application of a sufficiently strong electric field normal to the boundary aligns the anisotropic axis more or less perpendicular to the plate, except for a thin layer adjacent to the boundary in which the alignment adjusts rapidly to the orientation dictated by the surface. With an appropriate choice of Cartesian axes such that the z-axis is normal to the plates, the equations governing the response of the nematic can be Equations (16) and (17), this restricting the choice of surface alignment to some degree. From these it is soon apparent that one must include flow in any transient behaviour in order to avoid an overdeterminancy of the problem. Following the application of the field, we observe that the induced flow decays after an interval of time and the alignment attains its equilibrium configuration, given by the static solution of equation (17). Here, however, we consider the somewhat simpler problem of the relaxation of this alignment when the field is subsequently removed, this being more relevant for the following section.

Choosing the moment at which the field is removed as the zero of time and the origin of coordinates on the plate, the initial conditions for our problem are therefore

$$\theta(z, 0) = \theta_e(z), \qquad u(z, 0) = 0, \quad z > 0, \tag{18}$$

where $\theta_e(z)$ is solution of

$$2f(\theta)\theta'' + \frac{\mathrm{d}f(\theta)}{\mathrm{d}\theta}(\theta')^2 - 2\varepsilon_a E^2 \sin\theta\cos\theta = 0, \tag{19}$$

subject to

$$\theta_e(0) = \frac{\pi}{2}, \qquad \theta_e'(z) \to 0 \quad \text{as } z \to \infty, \tag{20}$$

this assuming parallel alignment at the surface. One can show that the solution θ_e of the above problem is zero at large distances from the plate, and for sufficiently strong fields remains close to zero until very near the plate where it rapidly adjusts to the value at the wall. To

describe the relaxation following the removal of the field one must solve the coupled partial differential equations (16) and (17) with E zero, subject to the boundary conditions

$$\theta(0,t)=\frac{\pi}{2}, \qquad u(0,t)=0, \quad t>0, \tag{21a}$$

$$\theta(z,t)\to 0, \qquad u(z,t)\to 0, \quad \text{as } z\to\infty,\ t>0, \tag{21b}$$

the latter appropriate at least for finite time.

Given the difficulties inherent in solving the above nonlinear problem, Clark and Leslie [11] idealise the above by replacing the initial conditions (18) by

$$\theta(z,0)=0, \qquad u(z,0)=0, \quad z>0, \tag{22}$$

and the Equations (16) and (17) by the linear system

$$\rho\dot{u}=\eta_c u''+\alpha_2\dot{\theta}', \qquad \gamma_1\dot{\theta}=K_3\theta''-\alpha_2 u', \qquad 2\eta_c=\alpha_4+\alpha_5-\alpha_2, \tag{23}$$

these the equations obtained from Equations (16) and (17) by replacing the variable coefficients by their values when θ is zero, but retain the boundary conditions (21a) and (21b). The solution of this new problem one assumes must be a good approximation to the solution of the original problem at least for the initial response.

This new problem rather invites a solution in terms of a similarity variable and therefore we choose

$$\theta=F(s), \qquad u=\left(\frac{k}{t}\right)^{1/2}G(s), \quad s=\frac{z}{2(kt)^{1/2}}, \quad k=\frac{K_3}{\gamma_1}, \tag{24}$$

the Equations (23) quickly yielding

$$F''+2sF'=\frac{2\alpha_2}{\gamma_1}G', \tag{25a}$$

$$G''+2\varepsilon(sG'+G)=\frac{\alpha_2}{\eta_c}(sF''+F'), \quad \varepsilon=\frac{\rho K_3}{\gamma_1\eta_c}, \tag{25b}$$

the prime now denoting differentiation with respect to the similarity variable s. Also the initial and boundary conditions (22), (21a) and (21b) lead to

$$F(0)=\frac{\pi}{2}, \qquad G(0)=0, \qquad F(s)\to 0, \qquad sG(s)\to 0, \quad \text{as } s\to\infty. \tag{26}$$

Integration of the first of the Equations (25b) gives

$$G'+2\varepsilon sG=\frac{\alpha_2}{\eta_c}sF', \tag{27}$$

the constant of integration zero on account of the conditions (26) for large s. Hence, eliminating F from equation (25a), we have

$$sG''+\left[2(\alpha+\varepsilon)s^2-1\right]G'+4\varepsilon s^3G=0, \quad \alpha=1-\frac{\alpha_2^2}{\gamma_1\eta_c}, \tag{28}$$

where the parameter α lies between zero and unity in view of the conditions (15). The above equation has solutions $\exp(-\lambda s^2)$ provided that the constant λ satisfies

$$\lambda^2 - (\alpha + \varepsilon)\lambda + \varepsilon = 0, \tag{29}$$

and hence one finds that

$$G(s) = A\exp(-\lambda_1 s^2) + B\exp(-\lambda_2 s^2), \tag{30a}$$

$$2\lambda_1 = (\alpha+\varepsilon) + \left[(\alpha+\varepsilon)^2 - 4\varepsilon\right]^{1/2}, \quad 2\lambda_2 = (\alpha+\varepsilon) - \left[(\alpha+\varepsilon)^2 - 4\varepsilon\right]^{1/2}, \tag{30b}$$

A and B arbitrary constants. By appeal to Equation (27) the solution subject to conditions (26) is

$$F(s) = \frac{\pi}{2}\frac{\left[(\lambda_1-\varepsilon)\mathrm{erfc}(\lambda_1^{1/2}s) - \left(\frac{\lambda_1}{\lambda_2}\right)^{1/2}(\lambda_2-\varepsilon)\mathrm{erfc}(\lambda_2^{1/2}s)\right]}{\left[(\lambda_1-\varepsilon) - \left(\frac{\lambda_1}{\lambda_2}\right)^{1/2}(\lambda_2-\varepsilon)\right]}, \tag{31a}$$

$$G(s) = \frac{\alpha_2(\pi\lambda_1)^{1/2}\left(\exp(-\lambda_1 s^2) - \exp(-\lambda_2 s^2)\right)}{2\eta_c\left[(\lambda_1-\varepsilon) - \left(\frac{\lambda_1}{\lambda_2}\right)^{1/2}(\lambda_2-\varepsilon)\right]}, \tag{31b}$$

giving the general solution to the reduced problem. Clearly, the induced flow is large initially, but soon decays.

For most nematics, the parameter ε is very small, largely because the coefficients of the energy function (4) are small compared with the viscous coefficients. As a consequence it is more than reasonable to assume that

$$\varepsilon \ll \alpha, \tag{32}$$

and in this event to first order in ε, the roots of Equation (29) are

$$\lambda_1 = \alpha, \qquad \lambda_2 = \frac{\varepsilon}{\alpha}. \tag{33}$$

If we employ this approximation, our solution (31a) and (31b) yields

$$\theta = \frac{\pi}{2}\mathrm{erfc}(\alpha^{1/2}s), \qquad u = \frac{\alpha_2}{2\eta_c}\left(\frac{\pi k}{\alpha t}\right)^{1/2}\left(\exp(-\alpha s^2) - \exp\left(-\frac{\varepsilon s^2}{\alpha}\right)\right), \tag{34}$$

from which one can more readily identify properties of the solution. In particular, it is clear that the flow is in the direction of the positive x-axis, since α_2 is negative. In physical terms the flow is in the direction in which the director is falling.

To close this section we note one further point, namely that neglect of the fluid inertia has minimal effect upon the above solution. In this event, if one sets ρ equal to zero in Equations (23), the above analysis becomes somewhat simpler to yield in the same manner

$$\theta = \frac{\pi}{2}\mathrm{erfc}(\alpha^{1/2}s), \qquad u = \frac{\alpha_2}{2\eta_c}\left(\frac{\pi k}{\alpha t}\right)^{1/2}\left(\exp(-\alpha s^2) - 1\right), \tag{35}$$

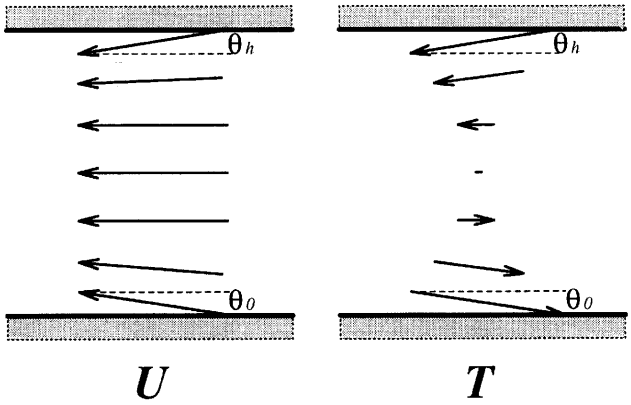

Figure 1. Uniform (U) and twisted (T) configurations.

which is simply the solution obtained by setting ε equal to zero in the above. The difference between the solutions (34) and (35) lies in the initial flow, not surprisingly, since it is no longer possible to satisfy the initial condition upon the flow when the inertial term is discarded.

4. Numerical study of reduced problem

For the device proposed by Dozov *et al.* [7] the two bistable textures considered are essentially a planar uniform one and a π-twisted one (see Figure 1). We may switch these two states by applying an electric field of appropriate strength across the cell, exploiting the fact that the anchoring strength at each surface is different. Thus, when the device is in its twisted state, an electric field of sufficient strength is applied perpendicular to the plates. The anchoring at the plate with weaker anchoring is then insufficient to maintain the twist and, when the field is removed, the cell relaxes back to the uniform state. Although this is not a simple process to model, the basis for the process is reasonably well understood.

The switch from uniform to twisted states is less obvious. Application of a sufficiently strong electric field across the cell in its uniform state induces a nearly perpendicular orientation of the director. When the field is removed, Dozov *et al.* [7] suggest that some form of hydrodynamic coupling between the plates occurs which can force the director to relax in opposite directions at either plate. This would eventually lead to a π-bend solution. However, there exists an energy argument which suggests that this structure is unstable and that it quickly transforms to the required π-twist structure. Modelling this change from uniform state to π-bend state may be achieved by employing the differential equations (16) and (17). In order to proceed further with these equations, we replace the set of six viscosity coefficients $\alpha_1 - \alpha_6$ in the equations (14)–(17) by one constant, employing the simplifications

$$\alpha_1 = \alpha_3 = \alpha_6 = 0, \qquad \alpha_4 = \alpha_5 = -\alpha_2 = \alpha, \tag{36}$$

and measuring this constant α, by setting it equal to the rotational viscosity γ_1. This reduction in the number of terms is justified if we consider the relative values of these coefficients for most nematics (see [21] and the references contained therein). This simplification reduces two of the expressions in (14) to

$$2g(\theta) = \alpha(1 + 2\cos^2\theta) \quad \text{and} \quad m(\theta) = -\alpha\cos^2\theta, \tag{37}$$

therefore reducing the complexity of differential equations (16) and (17).

The boundary and initial conditions for the flow are quite simple. One employs the usual no-slip condition for the velocity **v** and therefore

$$u = 0 \quad \text{on } z = 0, h, \tag{38}$$

and at $t = 0$ we require the flow to satisfy

$$u(z) = 0, \tag{39}$$

since initially the nematic is at rest. The boundary and initial conditions for the director angle θ are, however, considerably more complex. This is not unexpected, since the process which switches between uniform and twisted states originates in a region very close to the surface. With the anchoring at the top surface, $z = h$, assumed to be strong and fixed at an angle θ_h and the anchoring at the bottom surface, $z = 0$, assumed to be weak the boundary conditions may be assumed to be as follows

$$\theta(h, t) = \theta_h \tag{40a}$$

and

$$-f(\theta)\frac{\partial\theta}{\partial z} - A_0 \sin\theta\cos\theta + \eta\frac{\partial\theta}{\partial t} = 0 \quad \text{at } z = 0. \tag{40b}$$

Equation (40a), for the top boundary condition, is self explanatory, whilst (40b) is obtained from an adapted form of Jenkins and Barratt's surface equations [22]. The three terms in Equation (40b) represent bulk elastic, surface elastic and surface viscosity effects, respectively. The surface elastic term is obtained by use of the surface-anchoring energy per unit area

$$w_s = \tfrac{1}{2}A_0 \cos^2\theta, \tag{41}$$

where the anchoring strength at the bottom plate A_0 may be written as

$$A_0 = \frac{K_3}{l_0}, \tag{42}$$

where l_0 is the surface extrapolation length. The constant η is called the surface viscosity and has the dimensions of viscosity $\times$ length.

An initial condition for the director may be given by

$$\theta(z) = \theta_0 + \frac{z}{h}(\theta_h - \theta_0) \quad \text{for } z \in [0, h] \tag{43}$$

where θ_0 is the initial value of the director angle at $z = 0$. Although the director is unlikely to vary uniformly across the cell for an equilibrium solution – unless the solution is truly uniform – this seems not an unreasonable starting point.

Unfortunately, given the nonlinear nature of the differential equations which one is required to solve, it is not possible to provide useful exact analytic solutions. For this reason numerical methods are employed to deliver solutions to the differential equations (16) and (17) with the boundary and initial conditions (38)–(40b) and (43). These methods are based on the 'method

of lines' (see for example [23]) and convert the system of partial differential equations into a system of ordinary differential equations which proves simpler to solve.

Before proceeding with our numerical calculations it is necessary that we introduce values for the various parameters given in the equations. In this paper all values are given in cgs units and the material parameters used here are for the nematic liquid crystal 5CB at 32°C. ([24], [25]). However, other sets of material parameters have also been considered in the course of this investigation. The viscosity and elastic coefficients employed here are therefore

$$K_1 = 4 \times 10^{-7}, \qquad K_2 = 2 \times 10^{-7}, \qquad K_3 = 4{\cdot}85 \times 10^{-7} \quad \text{and} \quad \alpha = 0{\cdot}45. \tag{44}$$

Furthermore, the cell width used is 1μm, the value chosen for the surface viscosity is

$$\eta = \alpha \times 10^{-6}, \tag{45}$$

and, for reasons discussed in Section 3, we neglect the inertial term in the differential Equation (16). A numerical illustration of the acceptability of this final point is given in the following section. All other parameters will be defined for each separate example.

5. Study of solutions with the backflow effect

In this section we produce results which show that the suggested means of switching from uniform to twisted states by Dozov *et al.* [7] is correct. That is, the relaxation of the director at either plate from the near vertical – once the field has been switched off – is shown to be coupled and that it leads to a π-bend solution, which by an energy argument must become a π-twist solution.

In the first figure of this section representations of the director angle θ and flow component u are given at values across the cell and for increasing time t for the field switched on. These three-dimensional graphs give director and flow values at the spatial points

$$z = 0,\ 0{\cdot}1h,\ 0{\cdot}2h,\ 0{\cdot}3h, \ldots, 0{\cdot}9h,\ h, \tag{46}$$

for every 100 time-steps, as provided by the numerical routine. It is easy to see that across most of the cell the director angle approaches zero very quickly, differing only at the boundaries. At the $z = 0$ plate the weak anchoring necessitates the director lagging slightly behind that at the centre of the cell, whilst at the strongly anchored plate, $z = h$, it remains fixed at the angle θ_h. For the field switched on the flow is not particularly interesting, being almost symmetric across the cell and settling down to near zero as the director becomes normal to the plates.

Figure 3 shows θ and u values across the cell for increasing time after the electric field has been removed. From the first of these it is possible to see that the director does indeed tend towards a π-bend state between the plates, with the director angle near the strongly anchored top plate tending very quickly towards θ_h and that at the bottom plate moving in a slightly slower fashion towards $-\pi/2$. For the field off case the flow proves most instructive. Once the electric field has been removed the relaxation of the director near the strongly anchored top plate induces a flow at this plate which diffuses across the cell appearing with smaller magnitude at the $z = 0$ plate at a later time. It is this induced flow at the lower plate which affects the relaxation of the director there. Acting independently of any flow considerations the director at the weakly anchored surface would relax towards its original $\pi/2$ state. However, with the backflow the director is dragged past the vertical so that the angle θ becomes

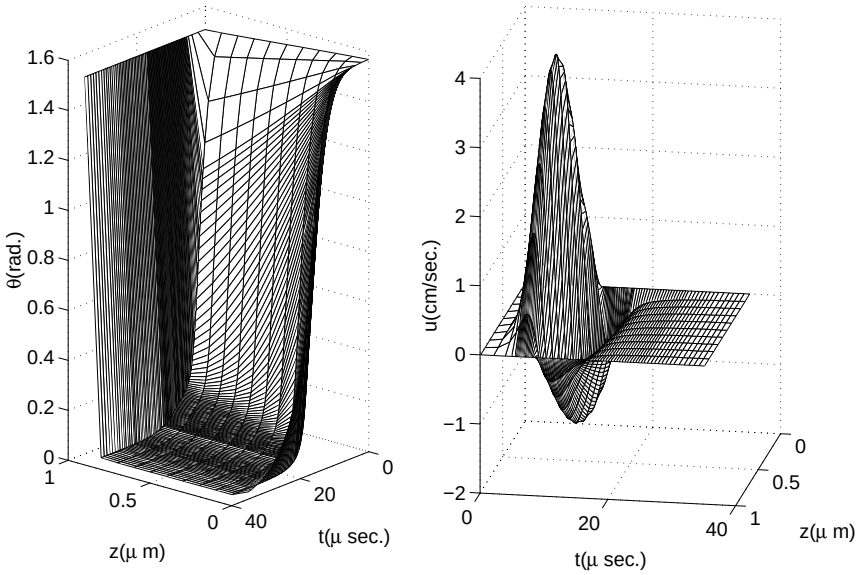

Figure 2. $\theta_h = 0{\cdot}48\pi$, $A_0 = 0{\cdot}1$, electric field on.

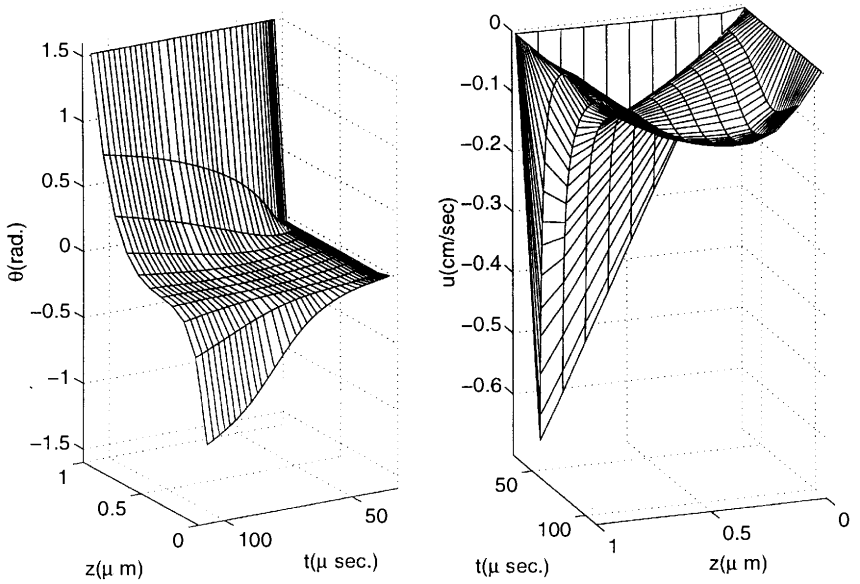

Figure 3. $\theta_h = 0{\cdot}48\pi$, $A_0 = 0{\cdot}1$, electric field off.

negative. Once this has happened any successive surface relaxation at the bottom plate sends the orientation towards $-\pi/2$.

When comparing the switching times of different solutions, we think it is useful to simply plot values for the director at three different points within the cell. Figure 4 shows such graphs for the example illustrated in Figures 2 and 3. The continuous line shows the director angle at $z = 0$ against time. The dotted and starred lines similarly show the director at $z = 0{\cdot}5h$ and $z = 0{\cdot}99h$, respectively.

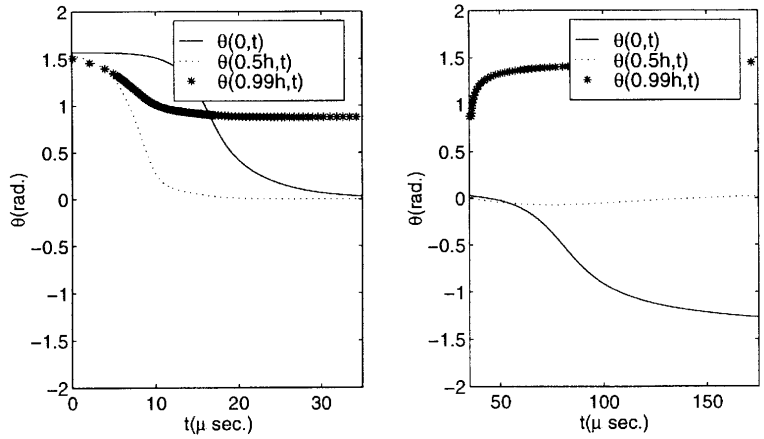

Figure 4. $\theta_h = 0{\cdot}48\pi$, $A_0 = 0{\cdot}1$, electric field on then off.

In order to compare solutions for different sets of parameters when the field has been removed, it is important that at that point the solutions are as close to each other as possible. Since the flow, and the director within the cell, tend towards zero at the end of the field on stage, and the angle θ_h is fixed at the top plate, the best way of ensuring closeness of solutions is requiring the angle θ at $z = 0$ to be the same for each compared solution when the field is switched off.

Figure 5 provides an illustration of how little difference inclusion of the inertial term in Equation (16) makes to the solution. The main reason that this simplification of the problem is desirable is that the numerical routine can require the taking of about 3000 times the number of numerical time-steps to solve the problem with the inertial term included in Equation (16) than without it. In this example the time scale begins at the point where the field is removed.

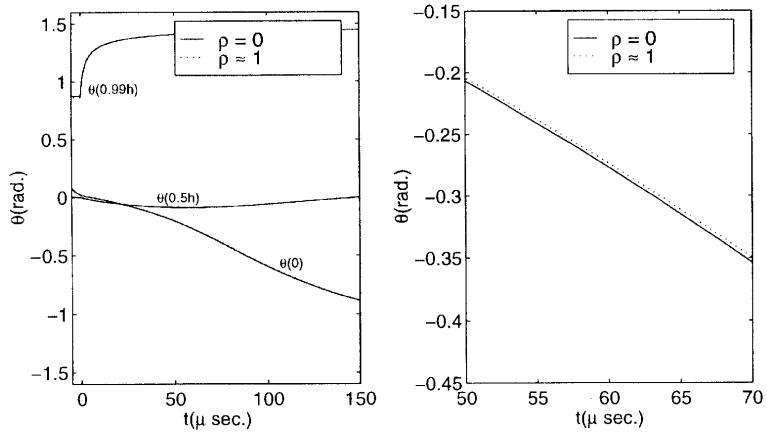

Figure 5. $\theta_h = 0{\cdot}48\pi$, $A_0 = 0{\cdot}05$. Comparison of solutions where $\rho = 0$ or $\rho \approx 1$ in differential equation (16). The first graph shows full solutions at three θ values. The second shows a detail of the θ solution at $z = 0$.

As increasing the switching speed of the proposed device would be advantageous, a fairly obvious step to take is to observe how changes in the anchoring strength A_0 at the weakly anchored surface change the solution. This is illustrated in Figure 6 where the value of the director angle at the $z = 0$ plate, once the field is removed, is given for different values of A_0.

Values of θ at the centre of the cell and at the top of the cell are very similar for the different A_0 values, and are therefore omitted from the figure. As A_0 increases the rate of change of θ at $z = 0$ increases in magnitude for the period of time where the switching speed is greatest. However, it can also be seen that the solution with the strongest weak anchoring shown in Figure 6 begins the switching process significantly later than the other three given solutions. The reason for this slowness of reaction is that it takes longer for the induced backflow to overcome the attempted relaxation of $\theta(0)$ towards $\pi/2$. Analogous to this result there is a strength of anchoring at the lower plate beyond which the solution will not switch to a π-bend solution. This is illustrated in Figure 7 where values of the director at $z = 0, 0{\cdot}5h$ and $0{\cdot}99h$ are given for different strengths of anchoring. For $A_0 = 0{\cdot}13$ the solution does tend towards a π-bend solution. However, with the anchoring strength increased to $A_0 = 0{\cdot}14$ the director at the lower plate relaxes back towards its original $\pi/2$ state before the backflow has a chance to effect it. As $t \to \infty$ this solution tends towards $\pi/2$ across the whole cell, except near the $z = h$ plate where the fixed director angle θ_h must be satisfied.

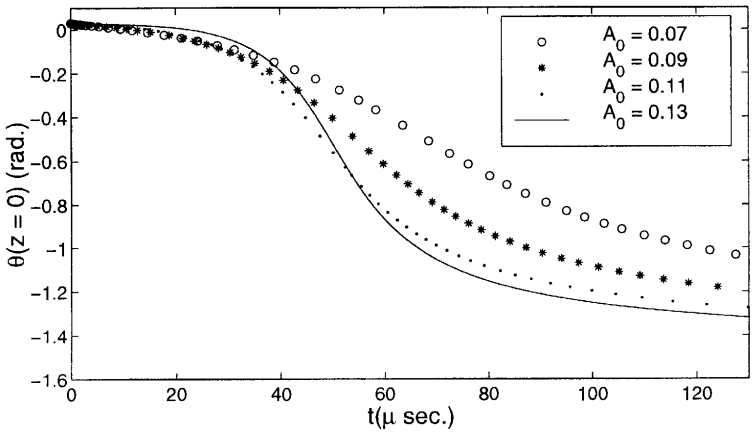

Figure 6. $\theta_h = 0{\cdot}48\pi$. Values of θ at $z = 0$ given for increasing A_0 values.

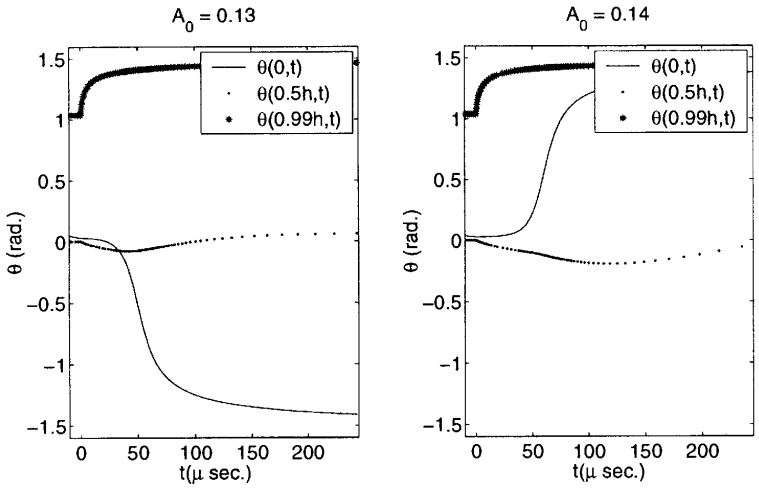

Figure 7. $\theta_h = 0{\cdot}48\pi$. For $A_0 = 0{\cdot}13$, the solution switches. For $A_0 = 0{\cdot}14$ the solution does not switch.

For the final figure in this paper we consider what consequence using strong anchoring at the top plate, and not weak anchoring similar to Equation (40b) for the $z = 0$ plate, has on the problem. In Figure 8 three solutions are shown with weak anchoring employed at both plates in comparison with one solution where the usual strong anchoring at the top plate (40a) is used. The weak anchoring boundary condition for the top plate is given by

$$f(\theta)\frac{\partial\theta}{\partial z} - A_h \sin\theta\cos\theta + \eta\frac{\partial\theta}{\partial t} = 0 \quad \text{at } z = h, \tag{47}$$

where the anchoring strength A_h is assumed to be greater than A_0. In this example A_0 is fixed at the value 0·1 and A_h is varied. One can see that, not surprisingly, the strong, infinite anchoring provides a limit for the wholly weakly anchored problem.

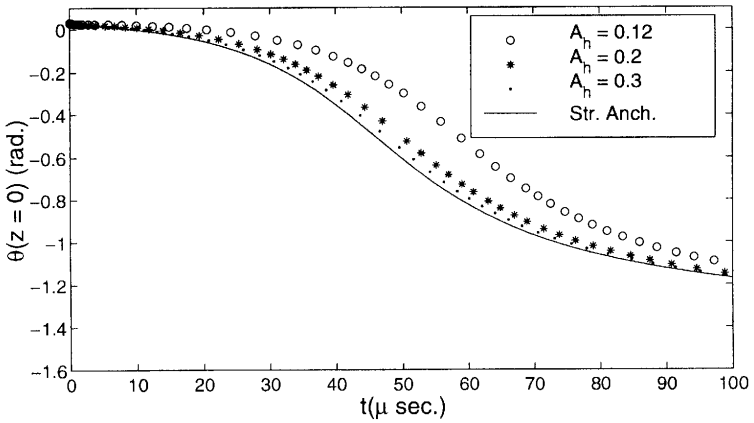

Figure 8. $\theta_h = 0{\cdot}48\pi$, $A_0 = 0{\cdot}1$. Comparison between different types of anchoring at the top surface.

6. Concluding remarks

The calculations described in this paper clearly demonstrate that the occurrence of backflow can lead to a rotation through π of the alignment in a planar nematic cell with a suitably small gapwidth and appropriate relative surface anchoring strengths. Since the splay and bend constants K_1 and K_3 are both larger than the twist constant K_2, this bend-splay deformation has a higher energy than a twist rotation through π, and therefore the nematic will ultimately relax to the lower energy state, presumably assisted by the chirality of the doped nematic. Given that the theory employed is well established, the above calculations do provide rather strong support for the mechanism put forward by Dozov, Nobili and Durand [7], although not providing details of the latter stage of the switching process.

It is naturally desirable to continue these calculations to describe the full switching process, but, since this entails a discussion of three-dimensional solutions for a chiral nematic, the increase in computational complexity presents a significant challenge. Equally, one would like to model the reverse switching from the π-twist to the uniform state, although the mechanism for this appears to be relatively straightforward [7]. These objectives having been achieved, there remains the problem of determining values of the material parameters that optimise the switching process.

References

1. C. J. Gerritsma, C. Z. Van Doorn and P. Van Zanten, Transient effects in the electrically controlled light transmission of a twisted nematic layer. *Phys. Lett.* 48A (1974) 263–264.
2. C. Z. Van Doorn, Transient behaviour of a twisted nematic liquid crystal layer in an electric field. *J. Phys. (Paris)* 36 (1975) C1 261–263.
3. C. Z. Van Doorn, Dynamic behaviour of twisted nematic liquid crystal layers in switched fields. *J. Appl. Phys.* 46 (1975) 3738–3745.
4. D. W. Berreman, Liquid crystal twist cell dynamics with backflow. *J. Appl. Phys.* 46 (1975) 3746–3751.
5. R. Barberi, M. Giocondo and G. Durand, Flexoelectrically controlled surface bistable switching in nematic liquid crystals. *Appl. Phys. Lett.* 60 (1992) 1085–1086.
6. G. P. Bryan-Brown, C. V. Brown, I. C. Sage and V. C. Hui, Voltage dependent anchoring of a nematic liquid crystal on a grating surface. *Nature* 392 (1998) 365–367.
7. I. Dozov, M. Nobili and G. Durand, Fast bistable nematic display using monostable surface switching. *Appl. Phys. Lett.* 70 (1997) 1179–1181.
8. J. G. McIntosh, P. J. Kedney and F. M. Leslie, Flow induced switching in a bistable nematic device. *Mol. Cryst. Liq. Cryst.* 330 (1999) 525–533.
9. J. L. Ericksen, Conservation laws for liquid crystals. *Trans. Soc. Rheol.* 5 (1961) 23–34.
10. F. M. Leslie, Some constitutive equations for liquid crystals. *Arch. Rat. Mech. Anal.* 28 (1968) 265–283.
11. M. G. Clark and F. M. Leslie, A calculation of orientational relaxation in nematic liquid crystals. *Proc. R. Soc. London A,* 361 (1978) 463–485.
12. P. G. de Gennes and J. Prost, *The Physics of Liquid Crystals, 2nd edn.* Oxford: Oxford University Press (1993) 597 pp.
13. S. Chandrasekhar, *Liquid Crystals, 2nd edn.* Cambridge: Cambridge University Press (1992) 460 pp.
14. F. M. Leslie, Continuum theory for liquid crystals. In: *Handbook of Liquid Crystals, Vol. 1; Fundamentals*. D. Demus, J. Goodby, G. W. Gray, H-W. Spiess, V. Vill (eds), Weinhein (Germany): Wiley-VCH (1998) pp. 25–39.
15. F. M. Leslie, Continuum theory for nematic liquid crystals. *Continuum Mech. Thermodyn.* 4 (1992) 167–175.
16. J. L. Ericksen, On equations of motion for liquid crystals. *Q. J. Mech. Appl. Math.* 29 (1976) 203–208.
17. C. W. Oseen, The theory of liquid crystals. *Trans. Faraday Soc.* 29 (1933) 883–899.
18. F. C. Frank, On the theory of liquid crystals. *Discussions Faraday Soc.* 25 (1958) 19–28.
19. F. M. Leslie, Some constitutive equations for anisotropic fluids. *Q. J. Mech. Appl. Math.* 19 (1966) 357–370.
20. O. Parodi, Stress tensor for a nematic liquid crystal. *J. Phys. (Paris)* 31 (1970) 581–584.
21. H. Kneppe and F. Schneider, Viscosity. In: *Handbook of Liquid Crystals, Vol. 2A; Low molecular weight liquid crystals I*. D. Demus, J. Goodby, G. W. Gray, H-W. Spiess, V. Vill (eds), Wiley-VCH. (1998) pp. 142–169.
22. J. T. Jenkins and P. J. Barratt, Interfacial effects in the static theory of nematic liquid crystals. *Q. J. Mech. Appl. Math.* 27 (1974) 111–127.
23. R. F. Sincovec and N. K. Madsen, Software for non-linear partial differential equations. *A. C. M. Trans. Math. Soft.* 1 (1975) 232–260.
24. H. Kneppe, F. Schneider and N. K. Sharma, Rotational viscosity γ_1 of nematic liquid crystals. *J. Chem. Phys.* 77 (1982) 3203–3208.
25. J. D. Bunning, T. E. Faber, P. L. Sherrell, The Frank constants of nematic 5CB at atmospheric pressure. *J. Phys. (Paris)* 42 (1981) 1175–1182.